Numerical Investigation of MHD Micropolar Fluid Flow Along an Inclined Permeable Surface with Variable Electric Conductivity and Variable Heat Flux

E. O. Fatunmbi[1] and A. O. Agbolade[2]
[1 -2]Department of Mathematics and Statistics, Federal Polytechnic, Ilaro, Nigeria
E-mail: [1]olusojiephesus@yahoo.com, [2]olumiya_agbolade@yahoo.com
Phone numbers: [1]08034013598, [2]08033185955
Corresponding author: olusojiephesus@yahoo.com

Abstract
This article presents hydromagnetic flow and heat transfer characteristics of micropolar fluid along an inclined permeable surface under the influences of variable electric conductivity, non-uniform heat generation/absorption, surface mass flux and variable heat flux condition. The model equations are developed as nonlinear partial differential equations and then transformed into a system of nonlinear ordinary differential equations by appropriate similarity transformation variables. Thereafter, a numerical solution is sought for the reduced governing equations via Runge-Kutta-Fehlberg integration scheme cum shooting techniques. The findings are both displayed on graphs and tables for the influences of the embedded controlling parameters. In the limiting situations, the results generated are in good agreement with the earlier published data in the literature. The results revealed that the momentum and thermal boundary layer thicknesses fall with a rise in the surface temperature parameter while the opposite occurs with a rise in both space and heat generation parameters
Keywords: Micropolar fluid; inclined sheet, permeable surface; non-uniform heat source/sink

1.0 INTRODUCTION

The dynamics of non-Newtonian fluids have gained prominence in the recent times owing to its practical scientific and industrial applications. Non-Newtonian fluids differ from Newtonian fluids most commonly due to the fact that the viscosity is dependent on the shear rate or shear rate history. These fluids do not follow the Newton's law of viscosity. Examples includes wall paint, blood, biological fluids (mucus, semen, synovia fluid), butter, cheese, etc. Micropolar fluids belong to non-Newtonian fluids due to its non-symmetric stress tensor. The model of micropolar fluids as well as the thermal conduction effects was initiated by Eringen (1966) as a sub-class of simple microfluid which was first proposed by Eringen (1964). Actually, this concept has been an active area of research for scientists and engineers because it offers a good mathematical model for studying the flow of complex and complicated fluids which includes suspension solution, fluids with certain additives, animal blood, liquid crystals, polymeric fluids and clouds with dust (Chen et al., *2011*; Hayat *et al.*, 2011). More areas of applications of micropolar fluids are polymer engineering, drug suspension in pharmacology, sediments in rivers, biological fluid modelling, crude oil extraction, food processing manufacturing and so on. In the physical description, micropolar fluids consists of rigid, randomly oriented (or spherical) particles suspended in a viscous medium, where particles deformation is ignored. Due to the complexity nature of such fluids individual fluid particles may vary in shapes and may shrink and/or expand, occasionally changing shapes and rotating independently of the rotational movement of the fluid (Lukaszewicz, 1999). Various transport activities that take place both in nature and industies include flow of fluids driven by buoyancy forces due to variations in density caused by variations in temperature. The use of magnetic field in engineering problems is crucial in various areas such as in plasma studies, nuclear reactors, oil exploration, geothermal energy extractions, MHD generators, and boundary layer control in the field of aerodynamic. In view of these immense applications, various reaserchers have invesigated such studies. (see Sreenivasulu et al., 2018; Fatunmbi and Fenuga, 2018, Fatunmbi and Adeniyan, 2018, Kumar, 2009, etc).

In engineering processes, suction/injection plays a key role for instance, it can is applicable in the design of thrust bearing and radial diffusion and thermal oil recovery. Iinjection is used in boundary layer control applications (e. g. film coating, polymer fiber coating and coating of wires), adding of reactants, prevention of corosion, reducing drag, etc. Also, suction can also be applied to remove reactants in chemical processes. To this end, Mukhopadhyay (2013) studied the effects of suction/injection on MHD boundary layer flow past an exponentially stretching sheet with thermal radiation while Hayat *et al.* (2010) included suction/injection effects while studying transfer of heat over a permeable stretching sheet. The aforementioned researches have been carried out with constant electric conductivity with or without uniform heat source/sink. However, the electric conductivity may vary with the fluid velocity and the heat source/sink can also be dependent not only on the temperature but on the space.(see Rahman, et al, 2009, Das 2011).

The aim of this study is to investigate boundary layer flow and heat transfer characteristics on an electrically conducting micropolar fluid over an inclined permeable surface with velocity dependent electric conductivity, variable magnetic field and variable heat flux. With the use of appropriate similarity transformation variables, the modelled nonlinear partial differential equations governing the problem are transformed into a system of nonlinear ordinary differential equations and then solved via the shooting method alongside Runge-Kutta-Fehlberg integration scheme. The effeects of the fluid controlling parameters embedded such as the suction/injection, variable heat flux exponent, micropolar parameters and inclination are presented and discussed.

2.0 Problem Formulation

Consider the flow and heat transfer of an electrically conducting, viscous and incompressible micropolar fluid along an inclined permeable sheet with Prescribed variable surface heat flux given as $-\kappa\frac{\partial T}{\partial y} = q_w = A\left(\frac{x}{L}\right)^n$, where A is a constant and n is power law temperature exponent parameter. The flow is assumed to be steady, two-dimensional and laminar with variable elcectric conductivity as well as variable applied magnetic field strength $\boldsymbol{B} = (0,\ B(x), 0)$ as respectively given in Eq. (6) and Eq. (7). The flow direction is assumed to be in the x axis direction which is taken along the surface with y axis normal to it. The magnetic Reynolds number is assumed to be small so that the induced magnetic field is negligible in comparison to the to the applied magnetic field. Darcy, Forchheimer resistance and thermal radiation terms are not considered in this study. In view of the aforementioned assumptions together with the Boussinesq and the usual boundary layer approximations, the governing equations of continuity, momentum, microrotation and energy equations are respectively modelled in Eqs. (1-4).

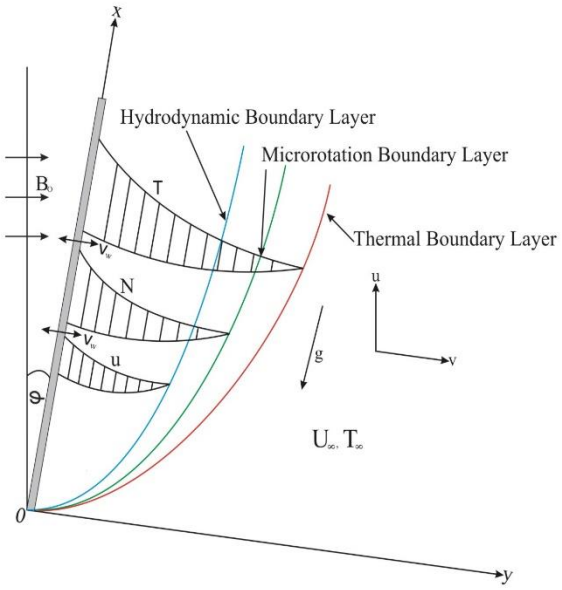

Fig. 1: Physical model and coordinate system

$$\frac{\partial u}{\partial x} + \frac{\partial v}{\partial y} = 0 \tag{1}$$

$$u\frac{\partial u}{\partial x} + v\frac{\partial u}{\partial y} = \left(\nu + \frac{\mu_r}{\rho}\right)\frac{\partial^2 u}{\partial y^2} + \frac{\mu_r}{\rho}\frac{\partial N}{\partial y} + g\beta_T\,(T - T_\infty)cos\varphi - \frac{\sigma_0'(B(x))^{\,2}}{\rho}u, \tag{2}$$

$$\rho j\left(u\frac{\partial N}{\partial x} + v\frac{\partial N}{\partial y}\right) = \gamma\frac{\partial^2 N}{\partial y^2} - \mu_r\left(2N + \frac{\partial u}{\partial y}\right), \tag{3}$$

$$u\frac{\partial T}{\partial x}+v\frac{\partial T}{\partial y}=\frac{\kappa}{\rho cp}\frac{\partial^2 T}{\partial y^2}+\frac{1}{\rho cp}(\mu+\mu_r)\left(\frac{\partial u}{\partial y}\right)^2+\frac{q'''}{\rho cp}. \tag{4}$$

The appropriate boundary conditions for Eqs. (1-4) are given by

$$y=0:\ u=0,\ v=V_w,\ N=-r\frac{\partial u}{\partial y}\ ,\ -\kappa\frac{\partial T}{\partial y}=q_w=A\left(\frac{x}{L}\right)^n\ , \tag{5}$$
$$y\to\infty:\ u=U_\infty=0,\ N=0,\ T\longrightarrow T_\infty.$$

Where u and v are the components of the velocity in x and y directions respectively, ν is the coefficient of kinematic viscosity, T is the fluid temperature, β_T is the thermal expansion coefficient. Similarly, $V_w\ is\ the$ suction/injection ($V_w<0$ is suction, ($V_w>0$ is injection), g is the acceleration due to gravity, ρ is the density, c_p the specific heat at constant pressure, κ is the thermal conductivity, N is the component of microrotation normal to $xy-$ plane and γ is the spin gradient viscosity, φ indicates the inclination angle, μ is the dynamic viscosity μ_r while is the vortex/microrotation viscosity. In the energy Eq. (4), the 4th term indicates the viscous dissipation effect while the 5th term represents the non-uniform heat source/sink. Also, r is the microrotation surface boundary parameter with $0\leq r\leq 1$. The case when $r=0$ corresponds to $N=0$ which indicates the vanishing of the spin on the boundary, also represents a strong concentration of the micro-particles such that the micro-particles close to the wall are unable to rotate as shown by Jena and Mathur (1981). The case $r=1/2$ indicates weak concentration of micro-particles and the vanishing of anti-symmetric part of the stress tensor (Ahmadi, 1976). The situation when $r=1$ represents the vanishing of a linear combination of spin, shearing stress and couple stress which is an indication of turbulent boundary layer flows as reported by Peddieson (1972).

It is to be noted also that when $\mu_r=0$, the velocity and microrotaion are decoupled and the macroscopic motion is unaffected by the microrotations. Similarly, when $\gamma=\mu_r=j=0$, the set of Eqs. (1-4) reduces to two-dimensional flow of incompressible Newtonian fluids.

The electric conductivity is assume to vary with the fluid velocity such as

$$\sigma_0'=\sigma_0 u, \tag{6}$$

and in the like manner, the applied magnetic field strength varies with x such as

$$B(x)=B_0 x^{-\frac{1}{2}}, \tag{7}$$

The 5th term in the energy equation (4) denotes the non-uniform heat source/sink and it is given as (see Rahman *et al*., 2009)

$$\mathrm{q}'''=\frac{\kappa}{2\nu x}[Q(T-T_\infty)+Q^*(T_w-T_\infty)\mathrm{e}^{-\eta}] \tag{8}$$

where $Q,\ Q^\star$ respectively represents the coefficient of space and temperature dependent heat source/sink. When $Q>0\ and\ Q^\star>0$ then, a case of heat source is implied, however, the a case of heat sink is indicated when $Q<0\ and\ Q^\star<0$.

The continuity Eq. (1) is satisfied by the introduction of the stream function defined by

$$u=\frac{\partial\psi}{\partial y},\ \nu-\frac{\partial\psi}{\partial x} \tag{9}$$

Also, Eqs. (2-5) are reduced to dimensionless ordinary differential equations by using the following transformation variables (see Mondal *et al*., 2017; Rahman *et al.*, 2009)

$$\psi=(2\nu U_0 x)^{\frac{1}{2}}f(\eta),\ \eta=y\left(\frac{U_0}{2\nu x}\right)^{\frac{1}{2}},$$
$$N=\left(\frac{U_0^3}{2\nu L}\right)^{\frac{1}{2}}g(\eta),\ T=T_\infty+(T_w-T_\infty)\theta(\eta) \tag{10}$$

Thus, after substituting Eq. (10) into Eqs. (2-5) and in view of Eqs. (6-8) the following nonlinear coupled ordinary differential equations are obtained:

$$(1+K)f''' + ff'' + Kg' + Gr\theta cos\varphi - Mf'^{2} = 0 \tag{11}$$

$$\left(1+\frac{K}{2}\right)g'' + fg' + f'g - 2K(2g + f'') = 0 \tag{12}$$

The energy equation (4) also becomes

$$\theta'' + \Pr(f\theta' - (2n+1)f'\theta + Q\theta) + PrEc\, f''^{2} + (Q\theta + Q^{*}e^{-\eta}) = 0. \tag{13}$$

The boundary conditions are also transformed to

$$\eta = 0:\ f' = 0,\ f = fw,\ g = -rf'', \theta = -1,$$
$$\eta \longrightarrow \infty:\ f' = 0,\ g = 0,\ \theta = 0. \tag{14}$$

Here, prime denotes differentiation with respect to η, $K = \mu_r/\mu$ is the material (micropolar) parameter, $M = \frac{2\sigma_0 B_0^2}{\rho}$ is the Magnetic parameter and $Gr = \frac{2xg\beta_T(T_w - T_\infty)}{U_0^2}$ is the Grashof number, $Pr = \frac{\mu cp}{\kappa}$ is the Prandtl number. Similarly, $Ec = \frac{U_0^2}{\rho\,(T_w - T_\infty)}$ stands for the Eckert number while $fw = -V_0\left(\frac{2}{U_0 v}\right)^{\frac{1}{2}}$ is the suction/injection parameter ($fw > 0$ suction , $fw < 0$ injection and $fw = 0$ corresponds to an impermeable sheet with $V_0 = V_w x^{-\frac{1}{2}}$.

3.0 Results and Discussion

The influences of various controlling parameters have been checked on the dimensionless velocity, temperature and microrotation profiles with the use of graphs and tables. Similarly, the reaction of the skin friction coefficient, Nusselt number and that of wall couple stress coefficient are tabulated with variations in the physical parameters. The default values adopted for computation in this study are: $K = 5.0,\ Gr = 10,\ M = 2.0, n = 0.2, Q = Q^{*} = 0.5,\ Ec = 0.02,$ $fw = 0.5, \varphi = 30°,\ Pr = 0.73$. The plots correspond to these values unless otherwise indicated on the graph.
The nonnlinear differential equations (11-13) together with the boundary conditions (14) constitutes a two point boundary value problem (BVP) which are solved using shooting iteration technique alongside Runge-Kutta-Fehlberg integration scheme. In the absence of the suction/injection parameter fw, Eckert number Ec and the variable heat flux exponent parameter n, the problem considered in this work reduces to that of Rahman *et al.* (2009). Hence, comparison of C_{fx} and Nu_x of this work with Rahman, *et al*. (2009) for variations in φ and M for both Variable Electric Conductivity (VEC) and Constant Electric Conductivity (CEC) are found to be in good agreement as recorded in Tables 1 and 2 respectively. This confirms the correctness of our code for this work. The quantities of engineering interest such as the skin friction coefficient Cf_x and the Nusselt number Nu_x (rate of heat transfer at the surface) are found out from the numerical computations.
Similarly, in Tables 1 and 2, we have compared the response of the Variable Electric Conductivity (VEC) and the Constant Electric Conductivity (CEC) on the skin friction coefficient Cf_x and the Nusselt number Nu_x for various values of inclination angle φ and the magnetic field parameter. It is evidently shown that the skin friction coefficient as well as the rate of heat transfer reduces with an increase in φ as seen in Table 1. However, both the shear stress at the surface Cf_x and the heat transfer Nu_x are higher for the case of Constant Electric Conductivity (CEC) than that of Variable Electric Conductivity (VEC).

In the like manner, Table 2 reveals that an increase in the magnetic field parameter M has a diminishing reaction on the skin friction coefficient Cf_x as well as on the rate of heat transfer at the surface for both cases of VEC and CEC. For physical quantities (Cf_x and Nu_x), the values of VEC are lower as compared with CEC.

Table 1**:** Comparison of values of C_{fx} and $N\,u_x$ with variation in φ

	Rahman, *et al*				Present Results			
	Cf_x	Cf_x	Nu_x	Nu_x	Cf_x	Cf_x	Nu_x	Nu_x
φ	VEC	CEC	VEC	CEC	VEC	CEC	VEC	CEC
0°	4.2424	4.2932	0.6403	0.6536	4.2440	4.2922	0.6397	0.6531
30°	3.9488	3.9859	0.6139	0.6245	3.9507	3.9851	0.6132	0.6240
45°	3.5731	3.5942	0.5777	0.5848	3.5752	3.5936	0.5770	0.5842
60°	3.0215	3.0233	0.5188	0.5201	3.0242	3.0229	0.5178	0.5194

Table 2**:** Comparison of values of C_{fx} and Nu_x with variation in M

	Rahman, *et al.*, (2009)				Present Results			
	Cf_x	Cf_x	Nu_x	Nu_x	Cf_x	Cf_x	Nu_x	Nu_x
M	VEC	CEC	VEC	CEC	VEC	CEC	VEC	CEC
0	4.2427	4.2427	0.6841	0.6841	4.2395	4.2395	0.6820	0.6820
0.2	4.1950	4.2079	0.6740	0.6768	4.1931	4.2055	0.6222	0.6750
0.5	4.1352	4.1606	0.6607	0.6665	4.1348	4.1591	0.6593	0.6651
0.8	4.0859	4.1185	0.6493	0.6570	4.0864	4.1175	0.6480	0.6568
1.0	4.0574	4.0927	0.6424	0.6509	4.0583	4.0919	0.6412	0.6500
1.5	3.9973	4.0353	0.6270	0.6371	3.9988	4.0346	0.6262	0.6364
2.0	3.9488	3.9859	0.6139	0.6245	3.9507	3.9851	0.6132	0.6240

Table 3**:** values of C_{fx} and $N\,u_x$ with variation in Gr when $n = 0, n = 0.7, n = 1.0$

	$n = 0$		$n = 0.7$		$n = 1.0$	
Gr	Cf_x	Nu_x	Cf_x	Nu_x	Cf_x	Nu_x
6.0	1.97650	2.06171	1.28545	1.67231	1.20207	1.56979
7.5	2.22249	1.94590	1.67052	1.49877	1.53972	1.39923
8.5	2.37773	1.88781	1.78826	1.45475	1.64862	1.35838
10.0	2.60069	1.81938	1.95605	1.40162	1.80357	1.30884

Table 3 depicts the influence of the Grashof number Gr on the surface shear stress Cf_x and the rate of heat transfer at the surface Nu_x for various values of the variable heat flux exponent n. It is clearly shown that an increase in Gr enhances the surface shear stress Cf_x while causing a reduction in the rate of heat transfer at the surface, i.e. Nu_x. However, with the imposition of the variable heat flux exponent n, the skin friction reduces better even with an increase in the Grashof number Gr. It is shown that the skin friction coefficient as well as the heat transfer rate is higher for the case of uniform heat flux ($n = 0$), hence, the application of variable heat flux can help to reduce the skin friction coefficient and as well lower the rate of heat transfer.

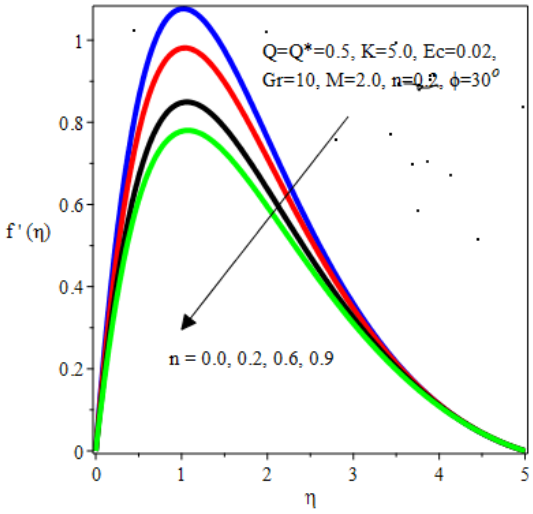

Figure 2: velocity profile for different values of n

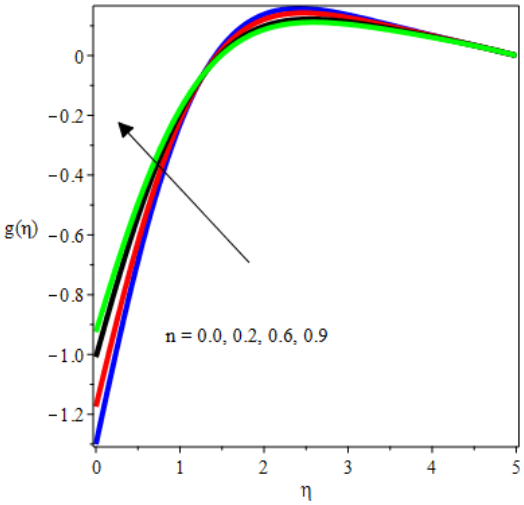

Figure 4: microrotation profile for different values of n

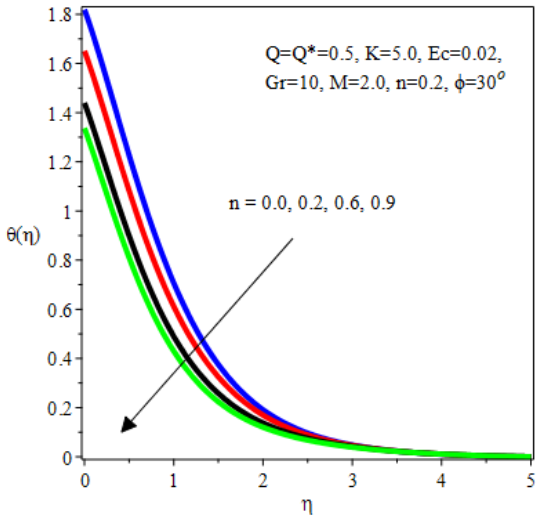

Figure 3: temperature profile for different values of n

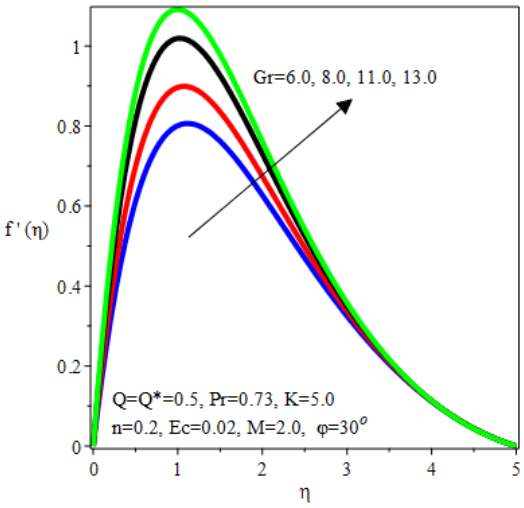

Figure 5: Variation of Gr on velocity profile

Figures 2-4 depict the effects of the heat flux exponent parameter n on the dimensionless velocity, temperature and microrotation profiles respectively. It is noticed in Figures 2-3 that both the velocity and temperature profiles decrease as the magnitude of n rises due to reduction in the hydromagnetic and thermal boundary layer thicknesses. On the contrary, the microrotation across the boundary layer appreciates as n increases in magnitude as displayed in Figure 4.

Figures 5-7 illustrate the influence of the Grashof number on the velocity, temperature and microrotation profiles. Evidently, the velocity increases as the magnitude of Gr rises as shown in Figure 5. Physically, Gr indicates the relative effect of the thermal buoyancy force to the viscous hydrodynamic force in the boundary layer. Hence, an increase in Gr enhances buoyancy forces which behaves as a favourable pressure gradient accelerating the fluid within the boundary layer. On the other hand, the temperature profiles depreciate as the magnitude of Gr increases as shown

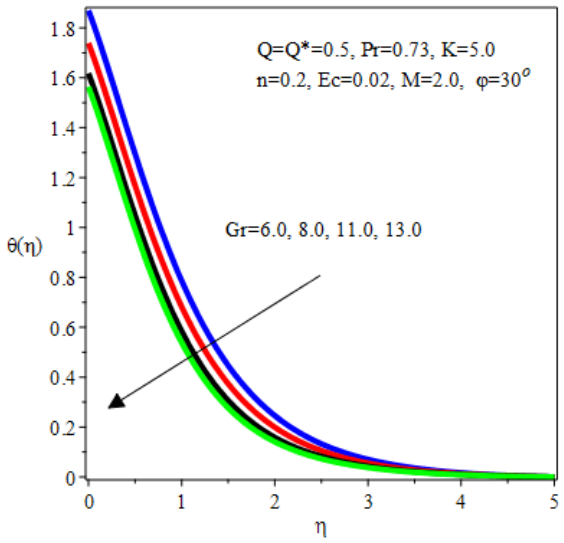

Figure 6: Variation of Gr on temperature profile

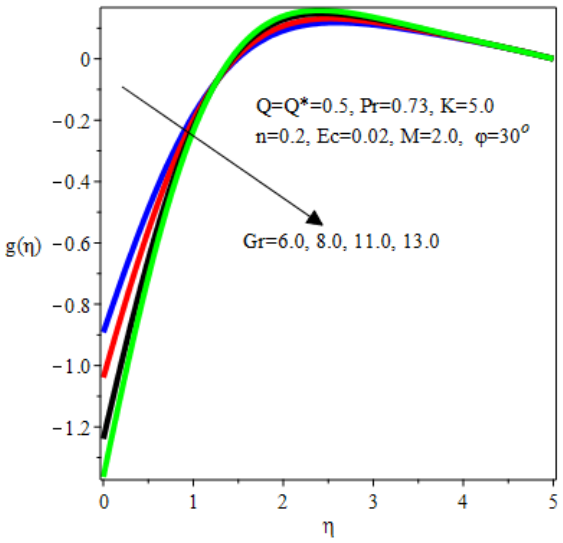

Figure 7: Variation of Gr on microrotation elocity profile

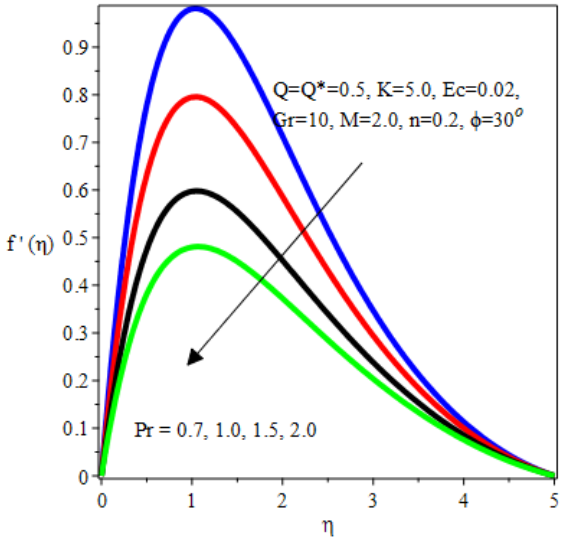

Figure 8: velocity profile for different values of Pr

in Figure 6. The influence of Gr is to decrease the microrotation profiles near the sheet but further away from the sheet, Gr has no influence on the profiles as depicted in Figure 7. The momentum and thermal boundary layer thicknesses are found to diminish with a rise in the Prandtl number Pr as displayed in Figures 8 and 9 respectively. These in turn reduces the velocity and also lowers the average temperature across the boundary layer while the microrotation profiles rises negatively as shown in Figure 10. Figures 11-12 depict the influence of the suction parameter $fw > 0$ on the velocity and temperature profiles respectively.

There is a fall in the velocity and temperature profiles with a rise in the $fw > 0$. An increase in $fw > 0$ causes a diminishing effect on both the velocity and temperature profiles due to the fact that the heated fluid is being pushed towards the sheet such that the fluid is brought closer to the surface which in turn leads to a reduction in the momentum and thermal boundary layer thicknesses.

Figures 14-16 shows the effects of the material parameter K on the velocity, temperature and microrotation profiles respectively.

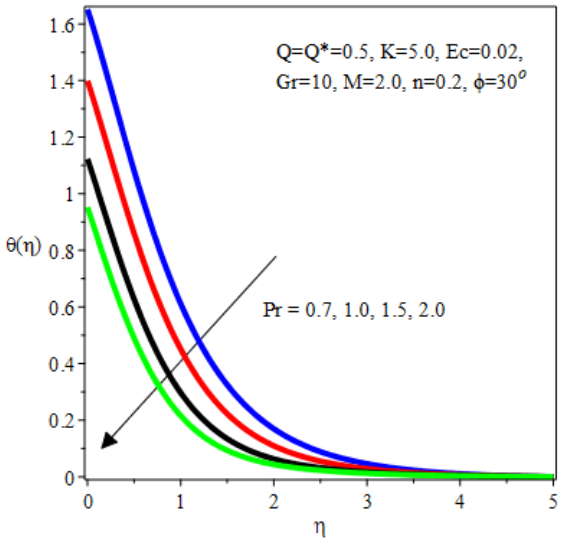

Figure 9: temperature profile for different values of Pr

For Figure 14, it is noticed that the velocity near the sheet decreases with a rise in K due to the reduction in the boundary layer thickness. However, further from the sheet the fluid motion accelerates. In the like manner, the thermal and microrotation boundary layer thicken with a rise in K leading to a rise in the temperature and the microrotation across the

boundary layer as respectively shown in Figures 15 and 16.

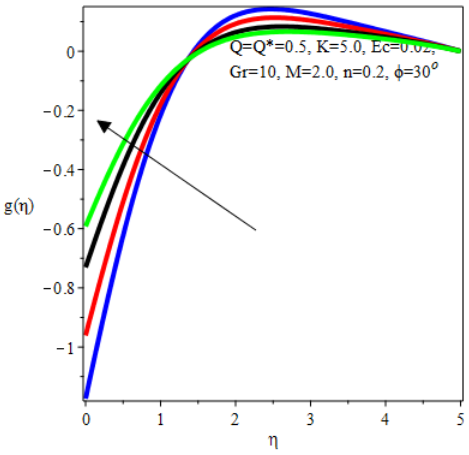

Figure 10: microrotation profile for different values of Pr

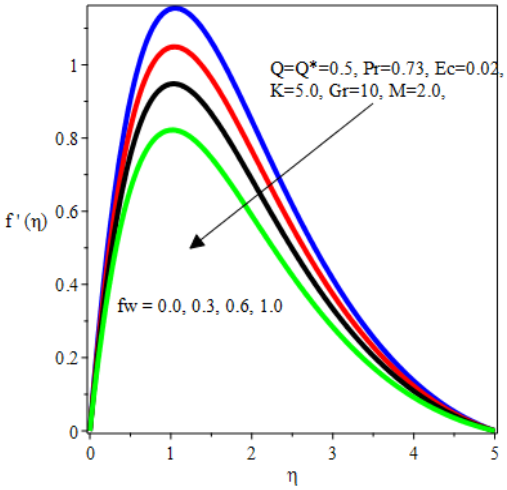

Figure 11: variation of fw on velocity profile

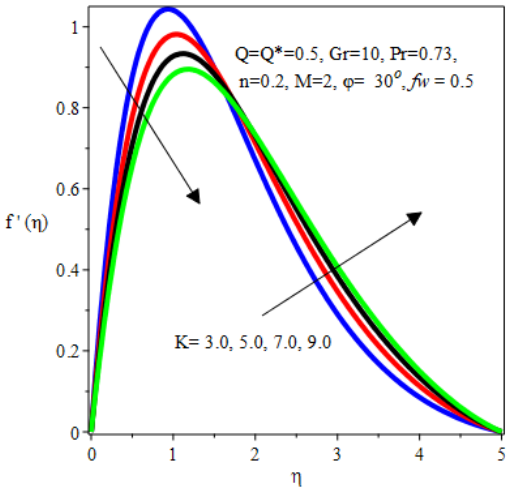

Figure 14: velocity profile for variation of K

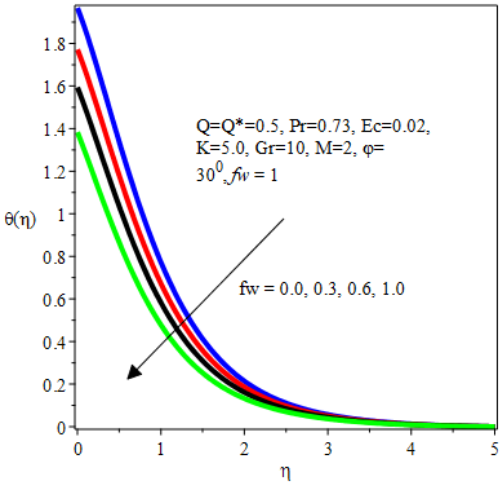

Figure 12: variation of fw on temperature profile

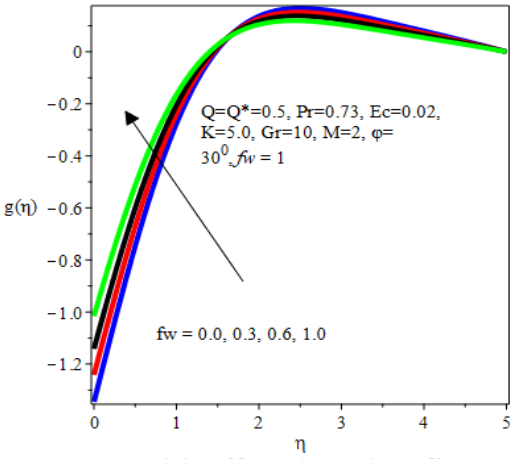

Figure 13: variation of fw on microrotation profile

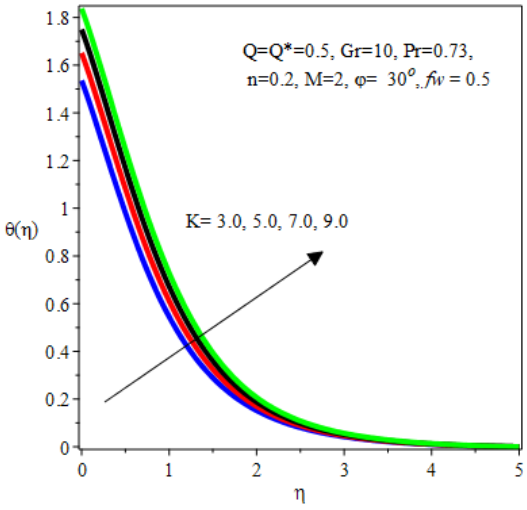

Figure 15: temperature profile for variation of K

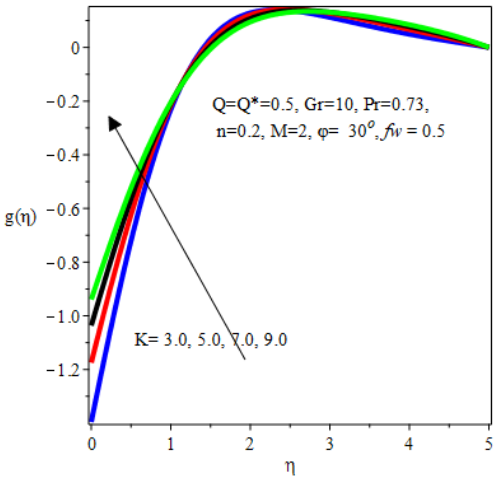

Figure 16: microrotation profile for variation of K

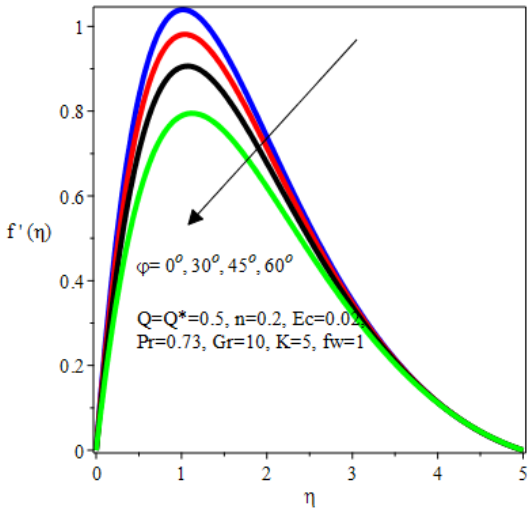

Figure 17: velocity profile for variation of φ

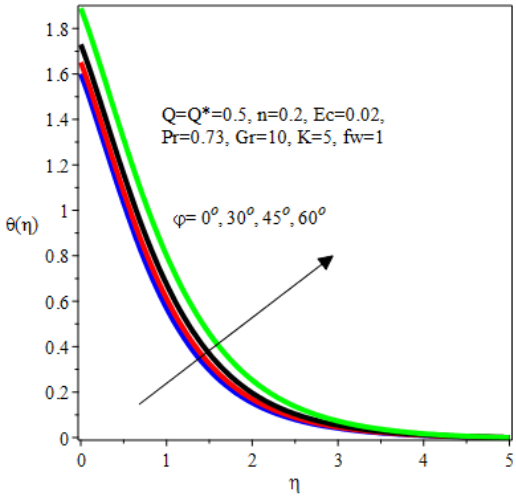

Figure 18: temperature profile for variation of φ

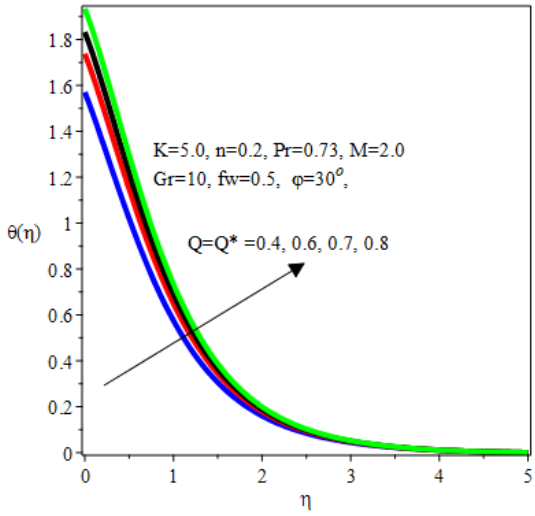

Figure 19: temperature profile for variation of Q=Q*

Figures 17-18 show the impact of the angle of inclination φ the velocity and temperature profiles. There is a fall in the velocity as seen in Figure 17. Higher velocity is observed when the surface is vertical because as the surface is inclined, the buoyancy driving influence is reduced by a factor of $\cos\varphi$. On the other hand, the temperature profile appreciates with a rise in φ as seen in Figure 18. In Figure 19, the thermal boundary layer thickens with a rise in the space/temperature-dependent heat source Q/Q^*. This in turn leads to a rise in the temperature profiles as energy is being generated with the imposition of Q/Q^*.

Conclusion

The present study has investigated flow and heat transfer characteristics of an electrically conducting micropolar fluid over an inclined permeable sheet with variable electric conductivity as well as variable magnetic field in the presence of non-uniform heat source/sink and surface mass flux. The system of ordinary differential equations governing the fluid flow and heat transfer has been integrated by shooting technique alongside Runge-Kutta-Fehlberg integration scheme while the effects of various thermo-pyhsical properties are presented through graphs and tables.

The following main points are deduced as conclusion of this study:

- The hydrodynamic as well as thermal boundary layer thickness diminishes with an increase in the magnitude of variable heat flux exponent parameter n, Prandtl number Pr and suction parameter fw.
- The temperature distribution across the boundary layer appreciates with an increase in the material parameter, K space/temperature-dependent heat source parameters $Q/Q^*$and inclination angle parameter φ while the reverse is the case with an increase in Grashof number Gr.
- Variable electric conductivity offers a better reduction in the viscous shear stress (Cf_x) than the constant electric conductivity whereas the rate of heat transfer across the surface (Nu_x) is higher for the constant electric conductivity.
- The skin friction coefficient as well as the Nusselt number drops with a rise in the magnitude of both magnetic field parameter M and inclination angle parameter φ.

References

Ahmadi, G. (1976). Self-similar solution of incompressible micropolar boundary layer flow over a semi-infinite plate, *Int. J. Engng Sci*, **14**, 639-646.

Chen, J., Liang, C. and Lee J. D. (2011). Theory and simulation of micropolar fluid dynamics, J. Nanoengineering and nanosystems, **224**: 31-39.

Das, K. (2012). Slip effects on heat and mass transfer in MHD micropolar fluid flow over an inclined plate with thermal radiation and chemical reaction, *Int. J. Numer. Meth. Fluids*, doi:10.2002/fd.2683.

Eringen, A. C. (1964). Simple microfluids., *International Journal of Engineering Science*, ***2***(2), 205-217.

Eringen, A. C. (1966). Theory of micropolar fluids, J. Math. Anal. Appl., **16**: 1-18.

Eringen, A. C. (1972). Theory of thermo-microfluids, Journal of Mathematical Analysis and Applications, **38**: 480-496.

Fatunmbi, E. O and Fenuga, O. J. (2017). MHD micropolar fluid flow over a permeable stretching sheet in the presence of variable viscosity and thermal conductivity with Soret and Dufour effects, *International Journal of Mathematical Analysis and Optimization: Theory and Applications*, **2017**: 211- 232.

Fatunmbi, E. O. and Adeniyan, A. (2018). MHD stagnation point-flow of micropolar fluids past a permeable stretching plate in porous media with thermal radiation, chemical reaction and viscous dissipation, *Journal of Advances in Mathematics and Computer Science*, **26**: 1-19.

Hayat, T., Shehzad, S. A. and Qasim, M. (2011). Mixed convection flow of a micropolar fluid with radiation and chemical reaction, *Int J. Numer Meth*, **67**:1418-1436.

Jena, S. K. and Mathur, M. N. Similarity solutions for laminar free convection flow of a thermomicropolar fluid past a non-isothermal flat plate, *Int. J. Eng. Sci.* **19**, 1431-1439.

Kumar, L. (2009). Finite element analysis of combined heat and mass transfer in hydromagnetic micropolar flow along a stretching sheet, *Computational Materials science*, **46**, 841-848.

Lukaszewicz, G. *Micropolar fluids: Theory and Applications*, 1st Ed., Birkhauser, Boston, 1999.

Mondal, H., Pal, D., Chatterjee, S., and Sibanda, P (2017). Thermophoresis and Soret-Dufour on MHD mixed convection mass transfer over an inclined plate with non-uniform heat source/sink and chemical reaction, *Ain Shams Eng. Journal*. doi.org./1016/j.asej.2016.10.015, 1-11.

Mukhopadhyay, S. (2013). Slip effects on MHD boundary layer flow over an exponentially stretching sheet with suction/blowing and thermal radiation, *Ain Shams Engineering Journal*, 485-491.

Peddieson, J and McNitt, R. P. (1970). Boundary layer theory for micropolar fluid, *Recent Adv. Enggng Sci*., **5**, 405.

Peddieson, J. (1972). An application of the micropolar model to the calculation of a turbulent shear flow, *Int. J. Eng. Sci*., **10:** 23-32.

Rahman, M. M., 2009. Convective flows of micropolar fluids from radiate isothermal porous surface with viscous dissipation and joule heating, *Commun Nonlinear Sci. Numer Simulat,14*, 3018-

Reddy, M. G. (2012). Heat generation and thermal radiation effects over a stretching sheet in a micropolar fluid, *International Scholarly Research Networks*, **2012**: 1-6. doi.org. /10.5402/2012/795814.

Sreenivasulu, P, Poornima, T. and Reddy, N. B. (2018). Internal heat generation effect on radiation heat transfer MHD dissipating flow of a micropolar fluid with variable wall heat flux, Journal of Naval Architecture and Marine Engineering, 1-12. doi.org//10.3329/jname.v15i1.19582.